RAFT Polymerization Kinetics: Combination of Apparently Conflicting Models

Dominik Konkolewicz, Brian S. Hawkett, Angus Gray-Weale, and Sébastien Perrier*

School of Chemistry, The University of Sydney, Chemistry Building F11, Sydney NSW 2006, Australia

Received February 20, 2008; Revised Manuscript Received May 15, 2008

ABSTRACT: We propose a model for the kinetics of reversible addition−fragmentation chain transfer (RAFT) polymerization. The essence of this model is that the termination of the radical intermediate formed by the RAFT process occurs only with the shortest active radicals. This model accounts for the absence of 3-armed stars predicted by other cross-termination models since the short radical makes a negligible difference to the overall molecular weight. The model is tested against experiments on styrene at 60 °C with cyanoisopropyl dithiobezoate (CPDB) as the RAFT agent. The predicted rate coefficients are consistent with slow fragmentation of the RAFT intermediate, and the overall concentration of radicals is consistent with ESR experiments. Overall, it demonstrates that the two conflicting models that have been proposed so far can actually coexist.

I. Introduction

In the past decade significant developments in radical polymerization have allowed an increase in the control over polymeric architecture. These developments are collectively known as "living radical polymerization", which include nitroxide-mediated polymerization (NMP),[1,2] atom-transfer radical polymerization (ATRP),[3,4] and reversible addition−fragmentation chain transfer (RAFT)-mediated polymerization.[5,6] Each of these methods gives narrow molecular weight distributions and good control of the polymer's molecular weight. It is argued that RAFT-mediated polymerization is the most versatile, since it can be adapted to the widest range of monomers.[7−10] RAFT polymerizations have been used to give a wide range of polymer architectures and topologies, including linear, block, gradient, star, and hyperbranched.[7,11−14] RAFT polymerization has also been used as a kinetic tool to study the chain length dependence of termination rates.[15−21] Despite the extensive use of RAFT in creating polymers of well-described architecture and molecular weight and many studies on the mechanism of the process, there is no consensus on the exact reaction mechanism for dithiobenzoate RAFT agents.[22]

RAFT polymerization kinetics have been studied by many researchers.[7,22−46] The methods and kinetic mechanisms are reviewed by Perrier and Takolpuckdee,[7] Barner-Kowolik et al.,[22] and Monteiro.[23] There are two predominant theories on the kinetic scheme, and each model gives conflicting predictions for the concentrations and lifetimes of various radical species.[22] The model of Barner-Kowollik et al.[24] assumes that the intermediate radical formed in the RAFT polymerization process is relatively stable and long-lived. The authors denote this model as the slow fragmentation model. This model predicts negligible termination of the intermediate radical and a large equilibrium constant ($\sim 10^{4-8}$) for the reaction of an active radical to a dormant/RAFT-stabilized radical.[24] In contrast, the model of Monteiro et al.[26] for RAFT polymerization kinetics assumes that there is significant cross-termination of the intermediate radical with other free radicals present in solution. The authors denote this model as the intermediate radical termination model. This model predicts equilibrium constants which are many orders of magnitude smaller than those of the slow fragmentation model ($\sim 10^{1-2}$), and because of the cross-termination and small equilibrium constant, it predicts a smaller overall radical concentration.[22,26] In addition to these models for RAFT polymerization, Buback et al.[28,29] propose an additional reaction step where there is a cross-termination between a propagating radical and a radical at the para position of a dithiobenzoate RAFT intermediate radical. Buback et al. predict that the 3-armed star polymer is attacked by another propagating radical, re-forming the RAFT intermediate radical and a terminated polymer of the two linear chains. This model succeeds in predicting the experimental observables, although the reaction mechanism has yet to be experimentally verified and requires the overcoming of many steric barriers and does not apply to RAFT agents such as carbazoles, which show similar behavior to dithiobenzoate RAFT agents.

In the literature, Monte Carlo methods,[27,31,32,47,48] method of moments,[33,34] and ordinary differential equations[24,25,30,40] have been used to describe the kinetics of RAFT polymerization. Coote et al.[36−38] have done theoretical work on the chain length dependent nature of radical addition/beta scission (fragmentation) rates. In addition to bulk systems, Monte Carlo simulations have also been used for RAFT emulsion systems.[32] These models generally give good agreement with experimental data, despite different assumptions in each of the two models (slow fragmentation vs intermediate termination).[22]

Despite the good agreement with conversion/polydispersity data, each model is in conflict with aspects of experimental results as well as agreeing with other aspects of the experiments. The intermediate termination model predicts radical concentrations in the correct order of magnitude as those observed experimentally (typically $10^{-7}-10^{-5}$).[22,41,49−52] However, the intermediate termination model gives equilibrium constants many orders of magnitude lower than those obtained from quantum calculations[36−38] and experiments.[53,54] In addition to the conflicting equilibrium constant predictions, the intermediate termination model predicts a significant number of 3-armed star polymers as products of the polymerization.[26] Although the star polymers have been detected in MALDI-TOF experiments specifically designed to detect them[55−57] and experiments using short polymer chains,[58] these 3-armed polymers have not being consistently observed in SEC experiments, despite the intermediate termination model predicting large quantities of these 3-armed star polymers.[22] On the other hand, the simple slow fragmentation model gives the correct distribution of polymer chains, since it does not predict 3-armed stars and gives equilibrium constants consistent with quantum calculations.[22,35−38] In contrast, the slow fragmentation model tends

* To whom correspondence should be addressed: e-mail s.perrier@chem.usyd.edu.au.

10.1021/ma800388c CCC: $40.75
Published on Web 08/16/2008

to give radical concentrations of $10^{-4}-10^{-3}$, which is many orders of magnitude higher than the experimentally observed concentrations.[22,41,49–52] For such kinetic models to realistically represent the synthetic process, the polymerization mechanism must be elucidated. In this paper we present a kinetic scheme which builds on the two predominant methods.

In our kinetic scheme we assume that the equilibrium constant is large (consistent with the slow fragmentation model), although we only include cross-termination between *short* radicals and the intermediate radical formed by the RAFT process. In other kinetic models the cross-termination between initiating/polymeric radicals and the RAFT intermediate is taken to be essentially constant or slowly vary with chain length of the active radical.[22,26] Although the review by Barner-Kowollik et al.[22] suggests that there may be a chain length dependence of the cross-termination rate, this is not explored in any depth. Furthermore, there have been no studies in the literature which propose a RAFT kinetic scheme that has very fast cross-termination of the RAFT intermediate with short chains and negligible long chain cross-termination.

In our kinetic scheme we assume that *only very short* radicals may terminate with the intermediate formed during in the RAFT process. This assumption is justified since the cross-terminated adduct of a RAFT intermediate radical, with a cyanoisopropyl radical, has been experimentally observed by MALDI-TOF.[59] This experimental finding is consistent with the essence of our model, which is that cross-termination occurs only between short radicals (in this paper we present the simplest case: initiator fragments and leaving groups such as the cyanoisopropyl radical) and the RAFT intermediate radical. A further argument for the cross-termination only occurring between short radicals and the RAFT intermediate is that termination events are diffusion controlled, with smaller radicals displaying much higher termination rate coefficients.[60] Specifically, the RAFT intermediate radical is expected to have significant steric hindrances, and we expect that only short radicals will be capable of diffusing near the RAFT intermediate radical and terminating. Since the model only includes cross-termination between short radicals and the RAFT intermediate, it accounts for the absence of 3-armed star polymers, since the third arm under these assumptions is a very short chain, which increases neither the polymer's molecular weight nor its hydrodynamic volume appreciably.

It is important that our model predicts an essentially unchanged hydrodynamic volume after cross-termination of the RAFT intermediate with short chains. This is because the predominantly used technique for characterizing linear polymers is size exclusion chromatography, which separates by hydrodynamic volume (not molecular weight).[61] Thus, if the cross-terminated product has essentially the same hydrodynamic volume as the product of conventional termination by combination for two polymer chains, then the cross-terminated product will not be experimentally distinguishable from the product of conventional radical−radical termination.

In this paper we outline our proposed kinetic scheme and show how we predict various properties such as the molecular weight distribution of polymer chains, etc. Once the theoretical system has been developed, we test the kinetic model against experiments on styrene to validate our model's assumptions and determine the consistency of our results with other studies on RAFT kinetics.

II. Experimental Section

A. Chemicals. Styrene monomer (Aldrich 99%), was purified by passing it through an alumina column to remove inhibitor. 2,2′-Azobis(isobutyronitrile) (AIBN, Aldrich) was recrystallized from ethanol and dried.

Table 1. Experimental Details of Polymerizations Performed

series	A	B	C	D
mass Sty (g)	5.4424	5.4481	5.4480	5.4453
moles Sty (mol)	5.2255×10^{-2}	5.2310×10^{-2}	5.2309×10^{-2}	5.2283×10^{-2}
mass AIBN (g)	3.5×10^{-3}	3.5×10^{-3}	3.5×10^{-3}	3.4×10^{-3}
moles AIBN (mol)	2.1×10^{-5}	2.1×10^{-5}	2.1×10^{-5}	2.1×10^{-5}
[AIBN]	3.6×10^{-3}	3.6×10^{-3}	3.6×10^{-3}	3.5×10^{-3}
mass CPDB (g)	4.6×10^{-3}	9.4×10^{-3}	1.88×10^{-2}	3.72×10^{-2}
moles CPDB	2.1×10^{-5}	4.2×10^{-5}	8.49×10^{-5}	1.68×10^{-4}
[CPDB]	3.5×10^{-3}	7.1×10^{-3}	1.42×10^{-2}	2.81×10^{-2}

B. RAFT Agent Synthesis. The RAFT agent 2-cyanoprop-2-yl dithiobenzoate, also known as cyanoisopropyl dithiobenzoate (CPDB), was synthesized by methods outlined in the literature.[62] The purity of RAFT agent was tested by NMR.

C. Size Exclusion Chromatography. Molecular weights were determined by size exclusion chromatography (SEC) at 40 °C on a system equipped with a Polymer Laboratories 10 μm guard column and Waters columns (HR 1-2-3-4) with both the differential refractive index detector (Shimadzu, RID-10A) and UV detector (Shimadzu, SPD-10A). Tetrahydrofuran was used as the eluent at a flow rate of 1 mL min $^{-1}$, and toluene was used as a flow rate marker. Polystyrene standards with a MW range of 526 000−682 g/mol were used for calibrations.

D. Polymerization. All reactions were performed in bulk styrene monomer at 60 °C. Four concentrations of RAFT were prepared: [CPDB] = 3.5×10^{-3}, 7.1×10^{-3}, 1.4×10^{-2}, and 2.8×10^{-2} M. The initiator concentration was [AIBN] = 3.5×10^{-3} M; see details in Table 1. Each stock solution (A−D) was prepared with 6 mL of styrene monomer then separated into 6 × 1 mL vials. Each vial was capped with a rubber septum placed in ice and then bubbled with nitrogen for 10 min to remove oxygen. Each vial was placed on a heating block set at 60 °C for their allotted time (2, 5, 9, 13, 18, and 24 h). After the alloted time the vials were placed in ice, and conversion determined by gravimetry. Molecular weights and polydisperities were determined by SEC.

III. Basic RAFT Kinetic Scheme

We present a kinetic scheme in this section which describes the evolution of the concentration of important species in the reaction mixture (e.g., monomer, initiator, etc.) over time. Note that this is an approximate kinetic scheme, and it neglects the many subtly different components in the solution. The focus of this section is to present the main features of our kinetic scheme, most notably that the cross-termination of the RAFT intermediate occurs only with *short* radicals as shown in Figure 3. In this paper we only consider cross-termination between the

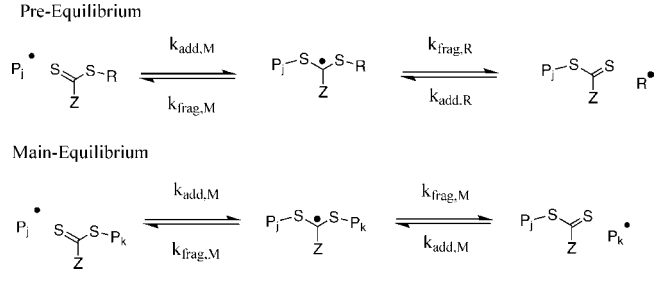

Figure 1. Mechanism of RAFT polymerization, where P_j and P_k represent polymer chains and R represents the RAFT agent leaving group.

shortest radicals, namely initiator fragments and radical leaving groups. The essence of our model would be unchanged if short oligomeric radicals (such as those with one or two monomers) were also included in the cross-termination reactions.

Initially, the only species present are the initiator [I_2], RAFT agent [X-R] (we use X to denote the dithioester + stabilizing group in the RAFT agent), and monomer [M]. In the approximation described in this section (denoted the *basic RAFT kinetic scheme*), only the most basic components of the reaction (active/dormant radicals, monomer, initiator, RAFT agent, etc.) are considered, with minimal chain length specifications. In the following section, an extension of this scheme is given, which allows the calculation of the full linear chain molecular weight distribution. By including considerations from the molecular weight distribution and the basic RAFT kinetic scheme, a very general model is built.

A. Reactions and Model Equations in the Basic RAFT Kinetic Scheme. Given the initial conditions and rate coefficients, the following kinetic scheme gives the time-dependent concentration of radicals (both active and RAFT stabilized), monomer, etc. In addition to time-dependent concentrations, this scheme can be used to deduce the evolution of the polymer's molecular weight distribution over time, as we show in the following section. The first reaction to consider is the initiation, or dissociation, of the initiator

$$I_2 \xrightarrow{k_d} 2f_I I^\bullet \tag{1}$$

where k_d is the dissociation rate coefficient, f_I is the initiator efficiency, and $I^\bullet$ represents the radical formed by the initiator. From this reaction scheme a differential equation that governs the time behavior of [I_2] is given.

$$\frac{d[I_2]}{dt} = -k_d[I_2] \tag{2}$$

Once the radical $I^\bullet$ forms, it may undergo the following reactions: propagation with the monomer M, with rate coefficient k_{p_I}, transfer to monomer, with rate coefficient k_{tr}, termination with other radicals, with rate coefficient k_t, deactivation with a dormant RAFT agent, with rate coefficient k_{add_I}, and activation of a dormant RAFT radical to give $I^\bullet$, with rate coefficient k_{frag_I}.

We make the approximation of only considering the radical species $I^\bullet$, $M^\bullet$, etc., ignoring the connectivity $I-M^\bullet$, etc. Although such chain length dependencies can be important in very short polymer chains,[36] for brevity and simplicity of the model, it is assumed that the pre-equilibrium and main equilibrium rate coefficients are sufficient to explain the kinetics of the long chain systems considered. RAFT agents are denoted as X-λ, where λ represents any species that can exist in an active radical form; in this model λ can be an initiator fragment I, a monomer M, or the RAFT agent's leaving group denoted R. $\lambda-X^\bullet-\theta$ denotes a dormant (RAFT-stabilized) radical. k_t is the termination rate coefficient, with chain length dependence of the termination rate coefficient included as follows:

$$k_{t_L} = k_{t_1} L^{-\alpha} \tag{3}$$

where L is the number-average degree of polymerization and is determined from the conversion and α is a power-law exponent, which gives the chain length dependence. In this work we use the assumption of a geometric mean for all chain length dependencies, that is, termination rate coefficient for chains of length j and k is given by $(k_{t_j} k_{t_k})^{1/2}$. This is especially important for conventional termination between polymeric chains and initiator fragments. For simplicity, in this work only a single power law is used for the chain length dependence of k_t, although Smith et al.[63] suggest that there

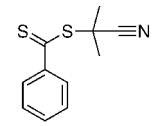

2-cyanopropan-2-yl benzodithioate

CPDB

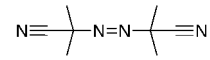

2,2'-Azobis(isobutyronitrile)

AIBN

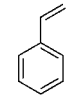

Styrene Monomer

Figure 2. Chemicals used in the RAFT polymerization.

are two power laws: an initial very steep power law followed by a small power law at high molecular weight. Since polymerizations under RAFT control approximately follow the trend $L \propto$ conversion, L is easily determined.

Generally a radical species $\lambda^\bullet$, which represents the species $I^\bullet$, $M^\bullet$, or $R^\bullet$, has the following reactions associated with it:

$$\lambda^\bullet + M \xrightarrow{k_{p_\lambda}} \lambda - M^\bullet = M^\bullet \tag{4}$$

$$\lambda^\bullet + M \xrightarrow{k_{tr}} \lambda + M^\bullet = M^\bullet \tag{5}$$

$$\lambda^\bullet + X-\theta \xrightarrow{k_{add_\lambda}} \lambda - X^\bullet - \theta \tag{6}$$

$$\lambda - X^\bullet - \theta \xrightarrow{k_{frag_\lambda}} \lambda^\bullet + X - \theta \tag{7}$$

$$\lambda^\bullet + \theta^\bullet \xrightarrow{k_{t_L}} \lambda - \theta \tag{8}$$

where θ also represents any species that can exist in an active radical form (I, M, or R) and may be the same or different from λ. The subscript λ on the rate coefficients indicates the potential dependence of each rate on the species λ. The final reaction to be considered is the cross-termination between the radical formed in the RAFT reaction and other radicals in solution. In this work it is assumed that only the shortest chains ($I^\bullet$ and $R^\bullet$) may terminate with the RAFT intermediate.

$$\lambda - X^\bullet - \theta + \omega^\bullet \xrightarrow{k_{t_{cross,L}}} \lambda - \underset{\omega}{\underset{|}{X}} - \theta \tag{9}$$

where ω is either an initiator fragment or a leaving group radical ($I^\bullet$ or $R^\bullet$). Chain length dependence in the cross-termination rate *could* be introduced by a power law although this is not included in the model since the exponent(s) are not well-known. Some dependence of the cross-termination rate is expected since the radical site on the RAFT intermediate becomes increasingly sterically hindered as the length of the polymers P_j and P_k in Figure 1 increases. These steric or segmental effects have been shown to follow power laws with an exponent of $\alpha \sim 0.16$ for conventional bimolecular termination,[21,63] although there is limited information about the short−long (midchain) terminations involved in this cross-termination reaction. Since the exact exponent α_c is not definitively known, we assume in this primary work that $\alpha_c \approx 0$. This assumption is equivalent to assuming that the cross-

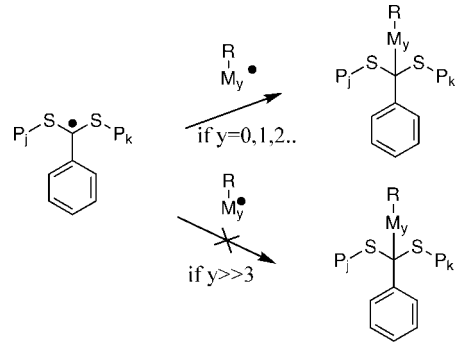

Figure 3. The kinetic scheme introduced in this paper, namely that cross-termination occurs only with short radicals $y \lesssim 3$, not long propagating radicals. In this paper we make the simplest approximation of only considering cross termination when $y = 0$.

termination rate is mainly determined by the diffusion properties of the short radical and the properties of the atoms near RAFT intermediate radical, which is a plausible approximation for very small radical species such as $I^\bullet$ and $R^\bullet$.

The reactions above (propagation, transfer, etc.) are for linear chain segments, which give following differential equation for the unreacted monomer species.

$$\frac{d[M]}{dt} = -(k_{p_I}[I^\bullet] + k_{p_M}[M^\bullet] + k_{p_R}[R^\bullet])[M] - k_{tr}([I^\bullet] + [M^\bullet] + [R^\bullet])[M] \quad (10)$$

Similarly, we set up the following reactions for the radical species:

$$\frac{d[I^\bullet]}{dt} = 2k_d f_I[I_2] - (k_{p_I} + k_{tr})[M][I^\bullet] - k_{t_1}[I^\bullet]([I^\bullet] + [R^\bullet]) - \sqrt{k_{t_1}k_{t_L}}[I^\bullet][M^\bullet] + k_{frag_I}\sum_{\lambda=I,M,R}(1+\delta_{I,\lambda})[I{-}X^\bullet{-}\lambda] - k_{add_I}[I^\bullet]\sum_{\lambda=I,M,R}[X{-}\lambda] - k_{t_{cross,1}}[I^\bullet]\sum_{all}[\lambda - X^\bullet - \theta] \quad (11)$$

$$\frac{d[M^\bullet]}{dt} = (k_{p_I}[I^\bullet] + k_{p_R}[R^\bullet])[M] + k_{tr}([I^\bullet] + [R^\bullet])[M] - k_{t_L}[M^\bullet][M^\bullet] - \sqrt{k_{t_1}k_{t_L}}[M^\bullet]([I^\bullet] + [R^\bullet]) + k_{fragM}\sum_{\lambda=I,M,R}(1+\delta_{M,\lambda})[M - X^\bullet - \lambda] - k_{addM}[M^\bullet]\sum_{\lambda=I,M,R}[X-\lambda] \quad (12)$$

$$\frac{d[R^\bullet]}{dt} = -(k_{p_R} + k_{tr})[M][R^\bullet] - k_{t_1}[R^\bullet]([I^\bullet] + [R^\bullet]) - \sqrt{k_{t_1}k_{t_L}}[R^\bullet][M^\bullet] + k_{frag_R}\sum_{\lambda=I,M,R}(1+\delta_{R,\lambda})[R - X^\bullet - \lambda] - k_{add_R}[R^\bullet]\sum_{\lambda=I,M,R}[X-\lambda] - k_{t_{cross,1}}[R^\bullet]\sum_{all}[\lambda - X^\bullet - \theta] \quad (13)$$

where $\delta_{i,j} = 1$ if $i = j$ or 0 otherwise. This allows for the fact that the species $[I{-}X^\bullet{-}M]$, $[M{-}X^\bullet{-}M]$, and $[R{-}X^\bullet{-}R]$ have two identical chains, either of which may fragment to give the active radical (see Figure 1). From this scheme the behavior of the RAFT agents and the dormant RAFT stabilized radicals are described as

$$\frac{d[X-\lambda]}{dt} = \sum_{\theta=I,M,R}(1+\delta_{\lambda,\theta})k_{frag_\theta}([\lambda - X^\bullet - \theta]) \quad (14)$$

$$-[X-\lambda](k_{add_I}[I^\bullet] + k_{add_M}[M^\bullet] + k_{add_R}[R^\bullet]) \quad (15)$$

$$\frac{d[\lambda - X^\bullet - \theta]}{dt} = -(k_{frag_\lambda} + k_{frag_\theta})[\lambda - X^\bullet - \theta] + (k_{add_\lambda}[\lambda^\bullet][X-\theta] + (1-\delta_{\lambda,\theta})k_{add_\theta}[\theta^\bullet][X-\lambda]) - k_{t_{cross,1}}[\lambda - X^\bullet - \theta]([I^\bullet] + [R^\bullet]) \quad (16)$$

for $\lambda, \theta = I, M, R$, accounting for the fact that $I{-}X^\bullet{-}M = M{-}X^\bullet{-}I$ to avoid double counting.

It is also important to track the number of terminations that have occurred. These termination events increase the population of dead chains and decrease the number of living chains. The number of chains that end in either termination by combination for two long chains or cross-termination between a RAFT intermediate and a short radical is given by

$$\frac{d[C]}{dt} = \frac{1}{2}f_c k_{t_L}[M^\bullet][M^\bullet] + k_{t_{cross,1}}([I^\bullet] + [R^\bullet])\sum_{all}[\lambda - X^\bullet - \theta] \quad (17)$$

where f_c is the fraction of terminations that end in combination. The factor of $^1/_2$ is placed since each combination event takes 2 radicals and forms 1 dead chain. The dead chains formed by combination/cross-termination have double the molecular weight of the living component chains. In addition to combination of long chains and cross-termination, dead chains of approximately the same molecular weight as the living chains may be produced by either short long termination or disproportionation between two long chains. Thus, the number of dead chains formed of approximately the same molecular weight as the living chains is given by

$$\frac{d[D]}{dt} = f_d k_{t_L}[M^\bullet][M^\bullet] + \sqrt{k_{t_L}k_{t_1}}([I^\bullet] + [R^\bullet])[M^\bullet] \quad (18)$$

where $f_d = 1 - f_c$ is the fraction of termination events that end in disproportionation.

IV. Extension: A Model for the Molecular Weight Distribution

A. Overview of Method. The methodology outlined earlier is generalized to a method which gives the full molecular weight distribution, rather than just the average molecular weight. A method is developed that uses the average concentrations of the radicals, monomer, RAFT agents, etc., to generate the distribution of the linear chains. The method used to generate the distribution of linear chain lengths is outlined in the following section.

Given the kinetics of RAFT polymerization, the majority of polymer chains are living, although in the dormant form. When a dormant radical decaps to give an active radical and a RAFT agent, the chains may propagate, terminate, etc. We use a theoretical method based on the probability of propagating terminating or recapping which is similar in approach to the Monte Carlo simulations of Prescott.[31] Although unlike the Monte Carlo approach, which simulates the events occurring to a large ensemble of representative particles, our approach makes statistical assumptions and parametrizations to give the distribution of the polymer's molecular weights. This theory for the molecular weight distribution is based on modeling the statistical average of *all possible* realizations, unlike the Monte Carlo approach which evolves all the polymers in an ensemble.

To model the evolution of the representative (ensemble averaged) polymer, we use the fact that the decapping of a polymer from the dormant to an active radical is a rare event. In a time step Δt we expect a living polymer to spend the majority of the time in the dormant state and a small time spent as an active radical. In a given a time interval Δt, the average number of decappings is denoted by μ_d. Since the decapping events are essentially random, the Poisson distribution is

assumed. This is because the Poisson distribution is often used to describe the number of observations/events that occur, given the independence of the events.[64] This distribution is characterized by one parameter: the mean (in our case μ_d). The Poisson distribution gives the probability of observing j events as follows:

$$P_d(j|\mu_d) = \frac{\exp(-\mu_d)\mu_d^{\,j}}{j!} \tag{19}$$

Once a dormant polymer has decapped and formed an active radical, there are several possible pathways. The first section considers the active chain propagating and increasing the linear chain length. Other events such as termination are accounted for in the simple kinetic scheme given in the previous section and the distribution of dead chains in the following section. The simple kinetic scheme is used as an input to our model for the molecular weight distribution. We assume that the probability of adding k monomers is given by a geometric distribution; therefore, the probability of adding k monomers during a single decapping is taken to be[64]

$$P_{add}(k|\mu_a, 1) = u^k(1-u) \tag{20}$$

where $u = \mu_a/(1 + \mu_a)$, with μ_a being the average number of monomers added during one deccaping, and the term of 1 refers to the fact this is the distribution of the number of added monomers in a *single decapping*. Distributions with forms similar to the one above have been shown to to be the relevant distribution in transfer-dominated systems[65,66] and pseudobulk RAFT emulsion systems.[32] Equation 20 gives the probability (u^k) of an active radical propagating k times before it transfers to a RAFT agent and is interpreted as the probability of observing k propagation steps before the transfer event occurs. In the majority of cases, systems under RAFT control have rates of transfer much faster than their rates of propagation; thus, it can be shown that in the limit of small u, P_{add} of eq 20 has the same form as the following Poisson distribution

$$P_{add_{poisson}}(k|\mu_a, 1) = \frac{\exp(-\mu_a)\mu_a^{\,k}}{k!} \tag{21}$$

where μ_a again is the mean number of monomers added by propagation during one decapping. For RAFT-controlled systems both the geometric distribution and the Poisson distribution give essentially the same limiting form; however, because of the consistent interpretation with other transfer-dominated systems, the geometric distribution is used throughout this work.

Along with monomer addition, an active radical may terminate with another active radical (by either combination or disproportionation), and we may observe cross-termination of the RAFT intermediate with a short radical. These termination events are included in the distribution of dead chains.

B. Modeling the Living Chain Length Distribution. The previous section specified the distribution of the number of decappings, and the distribution of propagation events, during a single decapping. It is now necessary to combine these effects to give the change in the molecular weight distribution of living chains within a given time interval Δt. To determine the change in the chain length distribution, the properties of the Poisson distribution are exploited as follows. Supposing in the time interval Δt there are j decappings. At each decapping the probability of adding k monomers is given by $P_{add}(k|\mu_a,1)$. It can be shown that after j decappings the probability of adding k monomers is given by

$$P_{add}(k|\mu_a, j) = u^k(1-u) \qquad \text{if } j = 1 \tag{22}$$

$$P_{add}(k|\mu_a, j) = \frac{u^k(1-u)^j}{j-1!}\prod_{i=1}^{j-1}(k+i) \qquad \text{if } j > 1 \tag{23}$$

where $u = \mu_a/(1 + \mu_a)$. This equation states that after more than one decapping the probability of adding $k \geq 1$ monomer increases, by the terms under the product. In RAFT systems the probability of adding monomers u is very small ($u \ll 1$ if transfer dominates propagation), and we may simplify the probability of addition $P_{add}(k|\mu_a, j)$ to the following approximate expressions:

$$P_{add}(0|\mu_a, j) \approx (1 - u \times j) \tag{24}$$

$$P_{add}(1|\mu_a, j) \approx (u \times j)(1 - u \times j) \tag{25}$$

$$P_{add}(k|\mu_a, j) \approx 0 \qquad \text{if } k > 1 \tag{26}$$

We observe the same approximate forms of P_{add} when we use the Poisson distribution, $P_{add_{poisson}}$ of eq 21.

Termination is not explicitly incorporated to this distribution of living chains, since we generally solve these systems with a small time step; thus, the number of terminations occurring in any one time step is quite small. Termination is included in an implicit manner since the concentration of radicals will change *between* time steps. In addition, termination events and their effect on the molecular weight distribution are incorporated in the next section by determining the distribution of *dead* chains, while this section focuses on the distribution of *living* chains.

The final contribution to consider is the randomness of the number of decappings. To obtain the distribution for the average number of propagation steps in the time interval Δt (denoted $P_{prop}(k|\mu_d, \mu_a)$), the distribution for the number of decappings ($P_d(j|\mu_d)$) is incorporated with the chain length increasing probabilities $P_{add}(k|\mu_a, j_d)$, as follows:

$$P_{prop}(k|\mu_d, \mu_a) = \sum_{j=0}^{\infty} P_d(j|\mu_d)P_{add}(k|\mu_a, j) \tag{27}$$

P_{prop} gives the distribution of the number of propagation steps (increases in the chain length) in a given time interval Δt. That is, $P_{prop}(k|\mu_d, \mu_a)$ is the probability of propagating $k = 0, 1, 2, 3,...$ monomers in the time Δt. P_{prop} is the weighted sum of the distribution of adding monomers after j decappings $P_{add}(k|\mu_a, j)$, where the weight is the probability of observing these j decappings. Equation 27 states that the probability of propagating k monomers in the time interval Δt is the probability of propagating k monomers under the assumption of 1 decapping, $P_{add}(k|\mu_a, 1)$, times the probability of observing 1 decapping, $P_d(1|\mu_d)$, *plus* the probability of propagating k monomers under the assumption of 2 decappings, $P_{add}(k|\mu_a, 2)$, times the probability of observing 2 decappings, $P_d(2|\mu_d)$, etc.

Before this time interval Δt the distribution of living linear chain lengths is assumed to be $P_{live}(k|t)$, where t is the time. Then the distribution of extended chain lengths at $t + \Delta t$ is the distribution $P_{live}(k|t)$ plus a contribution from P_{prop}, given by

$$P_{live}(k|t + \Delta t) = \sum_{i=0}^{k} P_{live}(k - i|t)P_{prop}(i|\mu_d, \mu_a) \tag{28}$$

for $k = 1, 2, 3,...$. This states that at time $t + \Delta t$ the proportion of living chains of length k is previous proportion of chains of length k, $P_{live}(k|t)$, *times* the probability of a chain not propagating at all, $P_{prop}(0|\mu_d, \mu_a)$, *plus* the previous proportion of chains of length $k - 1$, $P_{live}(k-1|t)$, *times* the probability of a chain propagating 1 monomer, $P_{prop}(1|\mu_d, \mu_a)$, etc., as well as extending polymers of length k to chains of length $k + 1$.

In addition to propagation, it is important to consider the contribution of initiator dissociation to the living chain distribution. These new chains comprise a fraction p_I of living chains:

$$p_I = \frac{2f_I([I_2]_t - [I_2]_{t+\Delta t})}{[N_{living}]_{t+\Delta t}} \tag{29}$$

where

$$[N_{\text{living}}]_t = \sum_{\lambda=I,M,R} [\lambda^\bullet]_t + \sum_{\lambda=I,M,R} [X-\lambda]_t + 2\sum_{\text{all}} [\lambda - X^\bullet - \theta]_t \tag{30}$$

Therefore, the new living chain distribution is given by the combination of those chains which have survived from the previous time (and possibly grown), and those new chains formed by dissociation of the initiator. The proportion of living chains of length zero, i.e. initiator/leaving group chains, is given by

$$P_{\text{live}}(0|t+\Delta t) = \frac{\sum_{\lambda=I,R} ([X-\lambda]_{t+\Delta t} + [\lambda^\bullet]_{t+\Delta t})}{[N_{\text{living}}]_{t+\Delta t}} + \frac{\sum_{\text{all}} (1 + \delta_{\lambda,\theta=I,R} - \delta_{\lambda,\theta=M})[\lambda - X^\bullet - \theta]_{t+\Delta t}}{[N_{\text{living}}]_{t+\Delta t}} \tag{31}$$

This is the sum of all RAFT agents with the zero length leaving group (initiator and RAFT leaving group), plus all active radicals of length zero, and all the zero length chains in the RAFT intermediates (where we double count by the δ, those which are $[I-X^\bullet-I]$, $[I-X^\bullet-R]$ and $[R-X^\bullet-R]$, $[M-X^\bullet-M]$). By including the p_I new chains formed by initiator dissociation, our model may be applied to systems where the concentration of initiator is relatively high.

The final term to consider is the propagation of chains of length 0 to unimers (polymers with a RAFT agent and one monomer). This can be determined as follows, in each time step a fraction p_I of all chains is formed of length 0. Thus, the number of chains of length 1, including those that propagate from length zero to length 1, is given by

$$P_{\text{live}}(1|t+\Delta t) = P_{\text{live}}(1|t) - (P_{\text{live}}(0|t+\Delta t) - P_{\text{live}}(0|t) - p_I) \tag{32}$$

Thus, the proportion of unimers, including the propagation of initiator/leaving groups, is the previous proportion of unimers, *plus* the change in the number of chains of length zero, since these chains have propagated. Equation 32 includes the number of propagated zero length chains that formed by initiator dissociation. Thus, if there is a steady proportion of chains of length zero, but constant initiator dissociation with proportion p_I of total chains, then there must be a constant increase in the number of chains of length 1, by propagation of the newly formed chains to unimers. This is captured by eq 32.

In our model, the overall growth in the distribution arising from propagation of polymeric chains is given by eq 28, while the proportion of chains of length zero is given by eq 31. There is also a correction for the number of chains propagating from length zero to length one given by eq 32. The initial condition is taken as a distribution where all the chains are of length zero; that is, we assume that at $t = 0$ $P_{\text{live}}(k|0) = \delta_{k,0}$ (all chains at $t = 0$ are living and are only a RAFT agent).

This distribution of linear chain lengths P_{live} depends on the choice of parameters: μ_a and μ_d, which must be consistently estimated. To estimate μ_a, we first note that propagation is *conditional* on the radical already being decapped; hence, μ_a is found by following the path of a single decapped radical. We first estimate the mean decapped lifetime for a radical. Once a radical has been decapped, it recaps when it reacts with a free RAFT agent. Similar to the Monte Carlo analysis of Prescott,[31] we estimate the mean decapped lifetime of a styrene monomer as

$$t_{\text{decap}} = \frac{1}{k_{\text{add}_M} \sum_{\lambda} [X-\lambda])} \tag{33}$$

For such a decapped radical, the mean number of propagations in this time is consequently given by

$$\mu_a = k_{p_M}[M]t_{\text{decap}} \tag{34}$$

The concentration of the decapped radical is not included because this mean is *conditional* on the fact that a radical *has already* decapped.

The last expression is the term for a *single* decapping. To estimate the number of decappings in the time interval Δt, we first find the mean number of decappings for a single particle in the time interval Δt and then correct for the proportion of chains in the dormant radical state (f_{dorm}). The mean number of decappings on a time interval Δt is

$$\mu_d = k_{\text{frag}_M} \Delta t f_{\text{dorm}} \tag{35}$$

where f_{dorm} is the proportion of dormant radical chains, given by

$$f_{\text{dorm}} = \frac{\sum_{\lambda=I,M,R} (1 + \delta_{\lambda,M})[M - X^\bullet - \lambda]_t}{[N_{\text{living}}]_t} \tag{36}$$

C. Distribution of Dead Chains. The previous section gave the distribution of living chains, whereas this section combines the results of the basic kinetic model that gives the concentration of dead chains and the model for the distribution of living chains to determine the distribution of dead linear chains. First, the fraction of living and dead chains is estimated as follows:

$$[N_{\text{living}}]_t = \sum_{\lambda=I,M,R} [\lambda^\bullet]_t + \sum_{\lambda=I,M,R} [X-\lambda]_t + 2\sum_{\text{all}} [\lambda - X^\bullet - \theta]_t \tag{37}$$

$$[N_{\text{dead}}]_t = [C]_t + [D]_t \tag{38}$$

$$f_{\text{live},t} = \frac{[N_{\text{living}}]_t}{[N_{\text{living}}]_t + [N_{\text{dead}}]_t} \tag{39}$$

where $f_{\text{live},t}$ is the fraction of living chains at time t. The species $[I^\bullet]_t$, $[X-I]_t$, etc., are determined from the differential equations in the basic kinetic scheme. In the time interval Δt there are the following increases in the number of dead chains

$$\Delta[C]_{t+\Delta t} = [C]_{t+\Delta t} - [C]_t \tag{40}$$

$$\Delta[D]_{t+\Delta t} = [D]_{t+\Delta t} - [D]_t \tag{41}$$

where $[C]$ is the concentration of dead chains formed by combination or cross-termination and $[D]$ is the concentration of dead chains formed by disproportionation or short−long termination.

Given that the distribution of dead chains at time t is given by $P_{\text{dead}}(k|t)$, the distribution of dead chains at time $t + \Delta t$ has a fraction of $[N_{\text{dead}}]_t/[N_{\text{dead}}]_{t+\Delta t}$ of dead chains formed up to time t. This fraction of $[N_{\text{dead}}]_t/[N_{\text{dead}}]_{t+\Delta t}$ follows the distribution $P_{\text{dead}}(k|t)$. In addition to this fraction of previously existing dead chains, there is an additional fraction $\Delta[C]_{t+\Delta t}/[N_{\text{dead}}]_{t+\Delta t}$ of chains formed in the time interval Δt, which forms either by combination of two long radicals or cross-termination between the RAFT intermediate and a short radical. These events give effectively double the molecular weight of the living chain distribution. The final component to the dead chain distribution formed in the time interval Δt is the increase in the number of short−long terminations and the number of long−long disproportionations. These additional disproportionation events occurring in the time interval Δt comprise a fraction $\Delta[D]_{t+\Delta t}/[N_{\text{dead}}]_{t+\Delta t}$ of the overall dead chain distribution.

Thus, the new dead chain distribution is the proportion of dead chains remaining from time t, *plus* the proportion of new chains formed by disproportionation, or short−long termination in the interval Δt, *plus* the dead chains formed by long−long combination or cross termination in the interval Δt. This gives the distribution of dead chains at time $t+\Delta t$

$$P_{\text{dead}}(k|t+\Delta t) = \frac{[N_{\text{dead}}]_t}{[N_{\text{dead}}]_{t+\Delta t}} P_{\text{dead}}(k|t) + \frac{\Delta[D]_{t+\Delta t}}{[N_{\text{dead}}]_{t+\Delta t}} P_{\text{live}}(k|t) + \frac{\Delta[C]_{t+\Delta t}}{[N_{\text{dead}}]_{t+\Delta t}} P_{\text{live}}(k|t) \circ P_{\text{live}}(k|t) \quad (42)$$

where $P_{\text{live}}(k|t) \circ P_{\text{live}}(k|t)$ represents the discrete convolution which accounts for the effective doubling of the molecular weight by the combination event. This is given below:

$$P_{\text{live}}(k|t) \circ P_{\text{live}}(k|t) = \sum_{i=0}^{k} P_{\text{live}}(k-i|t) P_{\text{live}}(i|t) \quad (43)$$

Equation 42 is comprised of three fractions: the first the dead chain distribution retained from the previous time period, $P_{\text{dead}}(k|t)$, *plus* a fraction $\Delta[D]_{t+\Delta t}/[N_{\text{dead}}]_{t+\Delta t}$ of chains formed by disproportionation, which have essentially the same molecular weight as the living polymers, $P_{\text{live}}(k|t)$, *plus* a fraction $\Delta[C]_{t+\Delta t}/[N_{\text{dead}}]_{t+\Delta t}$ of dead chains formed by combination/cross-termination which have double the molecular weight of the living chains, $P_{\text{live}}(k|t) \circ P_{\text{live}}(k|t)$.

Since the distribution of dead chains and the distribution of living chains are specified, the overall molecular weight distribution at time $t + \Delta t$ is determined as follows:

$$P_{\text{overall}}(k|t+\Delta t) = f_{\text{live},t+\Delta t} P_{\text{live}}(k|t+\Delta t) + (1 - f_{\text{live},t+\Delta t}) P_{\text{dead}}(k|t+\Delta t) \quad (44)$$

where f_{live} is the fraction of polymers that are living, given by eq 39. This derivation normalizes P_{overall} to unity. From P_{overall}, the number- and weight-averaged molecular weights are found as follows:

$$M_{\text{n},t+\Delta t} = M_0 \sum_k (k) P_{\text{overall}}(k|t+\Delta t) + M_{\text{RAFT}} \quad (45)$$

$$M_{\text{w},t+\Delta t} = \frac{{M_0}^2 \sum_k (k)^2 P_{\text{overall}}(k|t+\Delta t) + {M_{\text{RAFT}}}^2}{M_{\text{n},t+\Delta t}} \quad (46)$$

$$\text{PDI}_{\text{th},t+\Delta t} = \frac{M_{\text{w},t+\Delta t}}{M_{\text{n},t+\Delta t}} \quad (47)$$

where M_0 is the monomer's molecular weight and M_{RAFT} is the molecular weight of the RAFT agent.

D. Summary of Model. The inputs from the relatively simple coupled differential equations in the basic kinetic scheme are used to obtain the full molecular weight distribution, P_{overall}. The full molecular weight distribution may be determined with no further parameters and much less computational expense than approaches which use coupled differential equations for each polymer. The essence of the method is to use the basic kinetic scheme to update the living and dead polymer molecular weight distribution. The model uses the propagation rate to find P_{prop} the probability of increasing the length of a polymer chain by k units as follows:

$$P_{\text{prop}}(k|\mu_{\text{d}}, \mu_{\text{a}}) = \sum_{j=0}^{\infty} P_{\text{d}}(j|\mu_{\text{d}}) P_{\text{add}}(k|\mu_{\text{a}}, j) \quad (48)$$

where

$$P_{\text{d}}(j|\mu_{\text{d}}) = \frac{\exp(-\mu_{\text{d}}){\mu_{\text{d}}}^j}{j!} \quad (49)$$

and

$$P_{\text{add}}(0|\mu_{\text{a}}, j) \approx (1 - u \times j) \quad (50)$$

$$P_{\text{add}}(1|\mu_{\text{a}}, j) \approx (u \times j)(1 - u \times j) \quad (51)$$

$$P_{\text{add}}(k|\mu_a, j) \approx 0 \qquad \text{if } k > 1 \quad (52)$$

are the probability of decapping j times and the probability of adding k monomers in a single decapping where $u = \mu_{\text{a}}/(1 + \mu_{\text{a}})$ (note that the full formula for P_{add} is given in section IV.B). Once the probability of propagating k steps is determined, the distribution of living chains, P_{live}, is updated as follows:

$$P_{\text{live}}(k|t+\Delta t) = \sum_{i=0}^{k} P_{\text{live}}(k-i|t) P_{\text{prop}}(i|\mu_{\text{d}}, \mu_{\text{a}}) \quad (53)$$

The section on the living chain distribution also includes details for including the dissociation of the initiator, which gives new polymer chains.

In addition to the living chain distribution there is also a population of dead chains, which comprises of terminated chains. At each time step Δt the population of dead chains P_{dead} is updated as follows:

$$P_{\text{dead}}(k|t+\Delta t) = \frac{[N_{\text{dead}}]_t}{[N_{\text{dead}}]_{t+\Delta t}} P_{\text{dead}}(k|t) + \frac{\Delta[D]_{t+\Delta t}}{[N_{\text{dead}}]_{t+\Delta t}} P_{\text{live}}(k|t) + \frac{\Delta[C]_{t+\Delta t}}{[N_{\text{dead}}]_{t+\Delta t}} P_{\text{live}}(k|t) \circ P_{\text{live}}(k|t) \quad (54)$$

where $[N_{\text{dead}}]$ is the concentration of dead chains, $[C]$ is the concentration of chains that ended in combination/cross-termination, and $[D]$ is the concentration of chains that ended in disproporionation. The first term is the major component; it comprises dead chains which were retained from the previous time period. The new dead chain distribution comprises the old dead chain distribution *plus* a fraction of dead chains formed by termination by disproportionation, or short−long termination, *plus* a fraction of polymers formed by termination by combination or cross-termination. The living and dead chain distribution are combined to give the overall molecular weight distribution:

$$P_{\text{overall}}(k|t+\Delta t) = f_{\text{live},t+\Delta t} P_{\text{live}}(k|t+\Delta t) + (1 - f_{\text{live},t+\Delta t}) P_{\text{dead}}(k|t+\Delta t) \quad (55)$$

where f_{live} is the fraction of living chains.

The previous sections outline how to determine the parameters μ_{a}, μ_{d}, f_{live}, etc., using the basic kinetic scheme as an input. From P_{overall} the weight-averaged and number-averaged molecular weight and associated polydispersity index are determined. The quantities such as poly dispersity index are essential when fitting kinetic data to give rate coefficients.[25]

V. Kinetic Parameters and Solution Methods

A. Kinetic Parameters. In order to have a realistic theoretical model, the majority of parameters must be experimentally determined, and a minimal number of parameters may be fitted to the data. In this work the RAFT agent CPDB was chosen, since this RAFT agent has the cyanoisopropyl leaving group, which is the same group as the radical formed by the dissociation of AIBN. This effectively removes two parameters which would otherwise require estimation since $k_{\text{add}_I} = k_{\text{add}_R}$ and $k_{\text{frag}_I} = k_{\text{frag}_R}$. The other known rate coefficients used in this system are given in Table 2.

We make the assumption that cross-termination between the RAFT intermediate and a short radical is similar to the extrapolated rate of termination between two active radicals 3.9×10^8 L mol^{-1} s^{-1}. Similar assumptions are made in intermediate termination models, which assume the rate of cross-termination is the same as regular termination.[22,26] In this case we take the rate of cross-termination to be the extrapolated value of the regular termination; it is important to note that this value is in the same order of magnitude as other values of short short termination (such as the measured value of $k_{\text{t}} \approx 9 \times 10^8$ for two cumyl radicals at 50 °C[74]). This assumption is made to

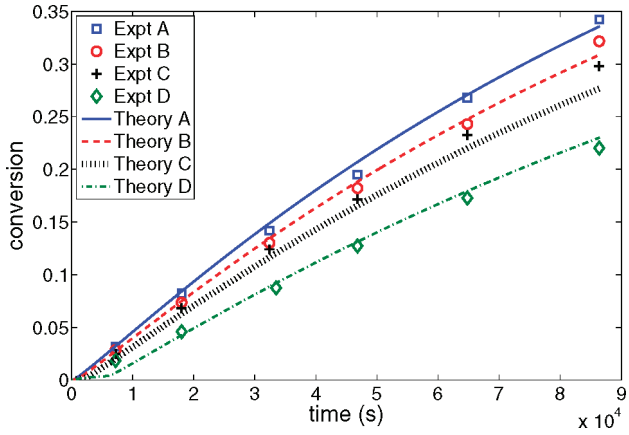

Figure 4. Experimentally determined conversion data and theoretical fit.

reduce the number of rate coefficients to estimate in our model, although in principle this parameter may also be estimated. No chain length dependence is included for the cross-termination rate; however, some effects are expected, since RAFT intermediates with long polymer chains are expected to give some steric hindrance to attack by short radicals.

In addition, k_{tr} is assumed ≈0, thus neglecting transfer to monomer. It is included in the reaction scheme for completeness. We also use the following relationship between the fraction of chains that terminate by combination and disproportionation $f_d = 1 - f_c$. To determine the L in the expression k_{t_L}, our model uses the fact that under RAFT control molecular weight grows linearly with conversion; thus

$$L = \frac{[M]_0 - [M]_t}{[X-R]_0} + 1 \tag{56}$$

B. Solution Methods. All equations were coded in the FORTRAN 90 language. The series of coupled differential equations in the basic kinetic scheme were solved by an Implicit Radau IIA (Order 5) method.[67,68] In fitting experimental data, a sample χ^2 value was generated by summing over all points in each series (A−D) by

$$\chi^2(k_{add_M}, k_{frag_M}, k_{add_I}, k_{frag_I}) = \sum_{A_i,B_i,C_i,D_i} (\nu_{th_i} - \nu_{dat_i})^2 + (PDI_{th_i} - PDI_{dat_i})^2 \tag{57}$$

where ν is the conversion given by $([M]_0 - [M]_t)/[M]_0$, and "th" refers to the theoretical prediction and "dat" the experimental data. The fit was optimized by minimizing the χ^2 value with the Powell's direction set minimization routine.[67]

VI. Results

The results of the experiments and the theoretical fit of the model to the experiments are shown in Figures 4–6, while the parameters used in the fit (best fit parameters) are given in Table 3. Figure 4 shows the conversion data, while Figure 5 shows the polydispersity data and Figure 6 shows the experimentally determined number-average molecular weights and the model's predictions for M_n, the number-average molecular weight.

Table 2. Kinetic Coefficients Used in Modeling the Styrene Polymerizations at 60 ° C

rate constant	value at $T = 333$ K	reference
k_d	9.53×10^{-6} s^{-1}	69
f_I	0.64	70
$k_{p_I} = k_{p_R}$	4130 L mol^{-1} s^{-1}	71
k_{p_M}	356 L mol^{-1} s^{-1}	72
k_{t_1}	3.904×10^8 L mol^{-1} s^{-1}	73
$k_{t_{cross,\,1}}$	3.904×10^8 L mol^{-1} s^{-1}	22, 26
k_{t_L}	$k_{t_1} L^{-0.16}$	63, 18
f_c	0.9	73
f_d	0.1	73

Table 3. Kinetic Coefficients for the RAFT Process Fitted in Modeling the Styrene Polymerizations at 60 ° C

rate constant	value from fit
k_{add_I}	1.80×10^7 L mol^{-1} s^{-1}
k_{frag_I}	4.03×10^2 s^{-1}
k_{add_M}	1.20×10^7 L mol^{-1} s^{-1}
k_{frag_M}	7.96×10^1 s^{-1}

In all cases, excellent agreement is seen between the experiments and the theoretical prediction, which serves as a confirmation of the model's validity.

The rate coefficients in Table 3 lead to large equilibrium constants, $K_M = 1.5 \times 10^5$ and $K_I = 4.4 \times 10^4$. These equilibrium constants are consistent with the slow fragmentation model for RAFT polymerization and suggest that the equilibrium is significantly in favor of the RAFT intermediate radical vs the RAFT agent and the free radical.

Because of the very large termination rate coefficient between short cyanoisopropyl radicals and the RAFT intermediate radical, there is a large number of cross-terminations, especially early in the polymerization, since all polymers are short and termination is facilitated. Because of the significant termination between cyanoisoproyl radicals and the RAFT intermediate radicals, the model predicts total radical concentrations in the order of 10^{-6}−10^{-5}, depending on the system. (The systems that have lowest radical concentrations are those which have the lowest ratio of RAFT:initiator.) In Figures 7 and 8 we show the simulated intermediate and propagating radical concentrations. The propagating radicals are generally in the order of 10^{-8} M, which is consistent with ESR data, while the intermediate radicals vary from 10^{-6} to 10^{-5} M from series A−D. These are broadly consistent with ESR experimental data, although our results are somewhat higher than those measured in experiments.

The new theoretical method of predicting the molecular weight distribution is tested against both existing theoretical methods (those which use the PREDICI program) and associated experiments. Since our model turns into the simple slow fragmentation model when $k_{t_{cross}} = 0$, we use the theoretical predictions and experiments of Barner-Kowollik et al.[24] as a benchmark for our model. For comparison to the experimental and theoretical molecular weight distributions, we used the same optimal rate coefficients that were used in the original work on cumyl dithiobenzoate.[24] In Figure 9 our model is compared against the theoretical model

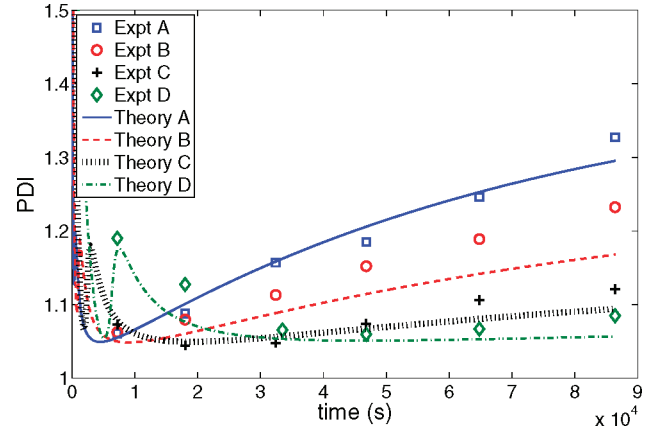

Figure 5. Experimentally determined poly dispersity index data and theoretical fit.

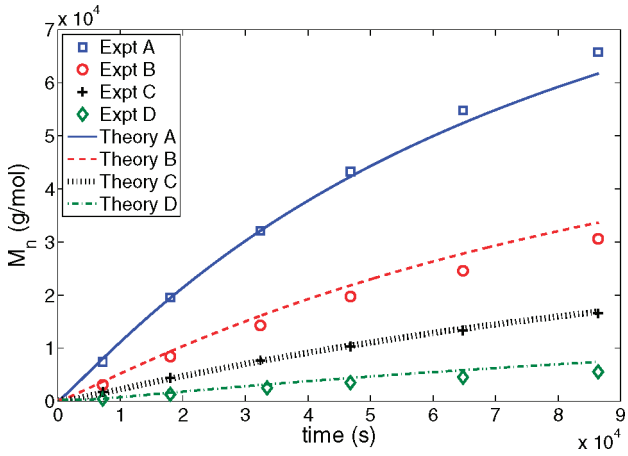

Figure 6. Experimentally determined number-average molecular weight data and theoretical fit.

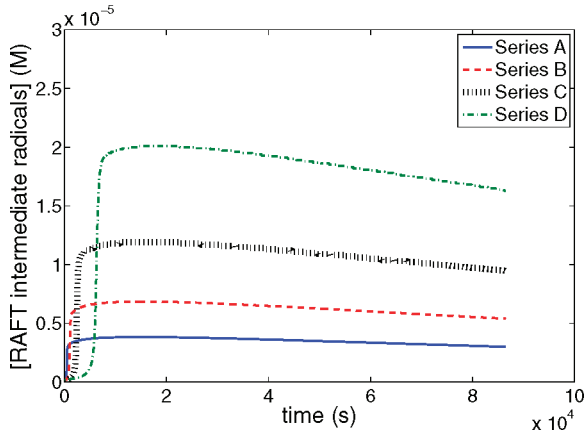

Figure 7. Simulated RAFT intermediate radical concentrations for series A−D. The radical concentrations are in the order of 10^{-6} and 10^{-5} M

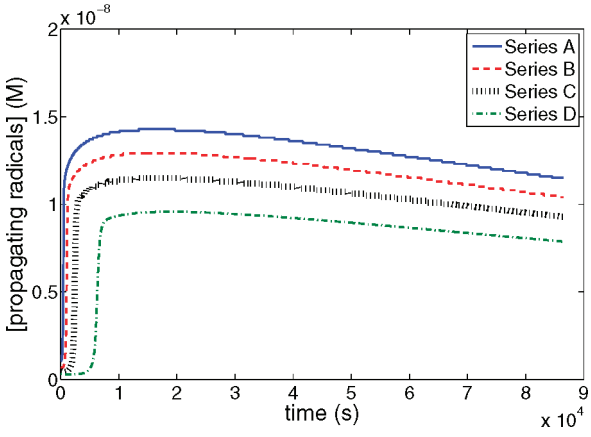

Figure 8. Simulated propagating radical concentrations for series A−D. In all cases the propagating radicals are in the order of 10^{-8} M.

of Barner-Kowollik et al.,[24] which uses the PREDICI software package, whereas Figure 10 compares our theoretical model against the experiments of Barner-Kowollik et al.[24] on cumyl dithiobenzoate. Our model agrees well with the theoretical model of Barner-Kowollik et al., suggesting that the method outlined is a good way of determining the molecular weight distribution. Furthermore, our model shows excellent agreement with the relevant experiments; in all cases our model shows a closer fit to the experimental data than the model of Barner-Kowollik et al.

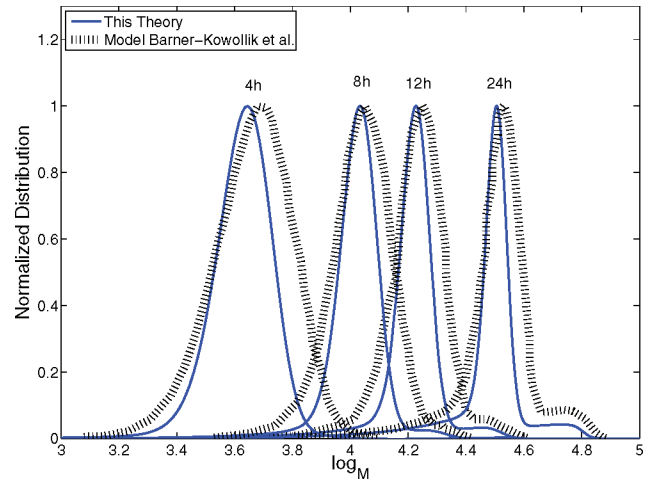

Figure 9. Comparison between the theory presented in this paper for the molecular weight distribution and the theoretical molecular weight distribution of Barner-Kowollik et al.[24] for cumyl dithiobenzoate.

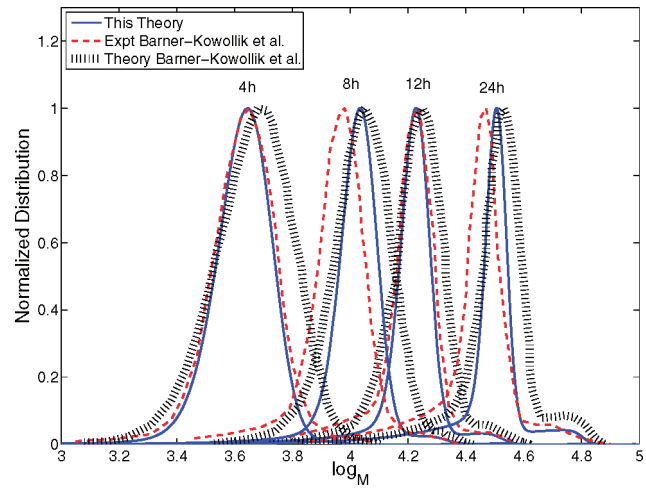

Figure 10. Comparison between the theory presented in this paper for the molecular weight distribution and the experimental molecular weight distribution of Barner-Kowollik et al.[24] for cumyl dithiobenzoate.

In Figures 9 and 10, we have benchmarked this theory against existing theoretical procedures and associated experiments and seen good agreement. In addition to the comparisons to previously published experiments and theories, we compare our model for the molecular weight distribution to our experimental molecular weight distributions. In Figure 11, we show the theoretical predictions of the molecular weight distribution and the experimental data for series C ([CPDB] = 1.42×10^{-2}), taken at 2, 9, and 24 h; the other times are similar and omitted for clarity. In all cases our theoretical curve predicts the correct molecular weight distribution (within errors associated with the method).

In addition to the fits, the sensitivity of the model was tested to variations in the rate coefficients and equilibrium constant from the fitted values. Figure 12 shows the behavior of our model when k_{frag} is increased/decreased by a factor of 10 (consequently, the equilibrium constant is also varied by a factor of 10). In series D we observe very large deviations from the experimental data/best fit curve as the vale of k_{frag} is increased/decreased. Although less pronounced, series A shows noticeable deviations from the experimental data as k_{frag} is varied. Since variations in k_{frag} cause large deviations in series D, and also the other series, there is strong evidence that the fitted equilibrium constant is appropriate to the system, under the model's assumptions. Since both the polydispersity data and

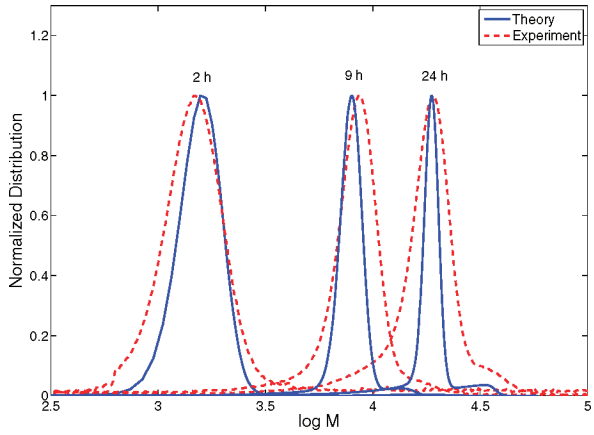

Figure 11. Comparison between the theoretical and experimental molecular weight distribution for the series C ([CPDB] = 1.42×10^{-2}) taken at 2, 9, and 24 h.

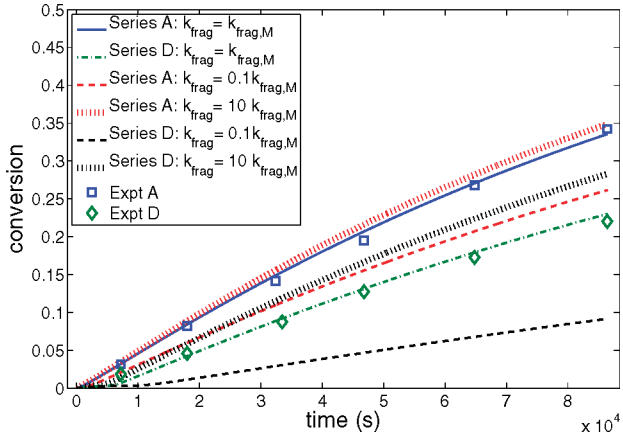

Figure 12. Behavior of the conversion predicted by our model the value of k_{frag} is varied for series A and series D. Significant deviations from the experimental data are observed in series A as k_{frag} is varied and very large discrepancies in series D.

the conversion data were fitted, the values in Table 3 are the best fit values of both k_{add_M} and k_{frag_M}.

The sensitivity of the model was also tested in regards to the exact value of the rate coefficient k_{add} in the main equilibrium. The value of k_{add} was decreased by 1 and 2 orders of magnitude from its best fit, while keeping the value of the equilibrium constant unchanged (by also decreasing k_{frag} by the same factor). Minimal difference was observed in the conversion in this sensitivity analysis since the conversion mainly varies with cross-termination rate and equilibrium constant.[25] However, deviations were observed in the theoretical PDI as seen in Figure 13 for series A and D, especially as k_{add} was decreased by 2 orders of magnitude. Even as k_{add} was decreased by 1 order of magnitude, the behavior of the PDI was influenced away from the experimental data in both series A and D. From this sensitivity analysis we argue that our estimated value of k_{add} is correct to within about 1 order of magnitude. It should be noted that further increasing k_{add} slightly lowered the PDI away from the experimental data.

The final analysis performed was the sensitivity of the intermediate radicals to variations in k_{frag} (variations in the equilibrium constant). In Figure 14, we observe that the radical concentration is inversely proportional to the equilibrium constant for both series A and series D. It is important to note that decreasing the equilibrium constant by 1 order of magnitude does decrease intermediate radical concentrations; however, the conversion values cease being consistent with the experimentally observed ones as seen in Figure 12.

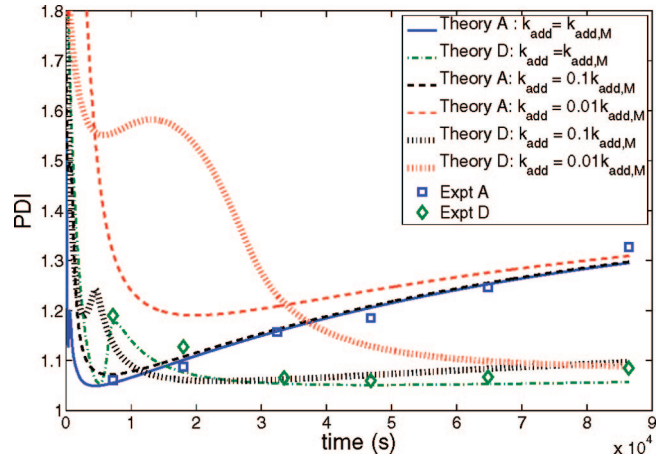

Figure 13. Comparison between the experimental and simulated PDI as the value of k_{add} is varied from its best fit value, while keeping the overall equilibrium constant unchanged. Decreasing k_{add} by 1 order of magnitude worsens the fit in both series A and D, while decreasing k_{add} by 2 orders of magnitude destroys the fit in series D, and shows significant discrepancy in series A.

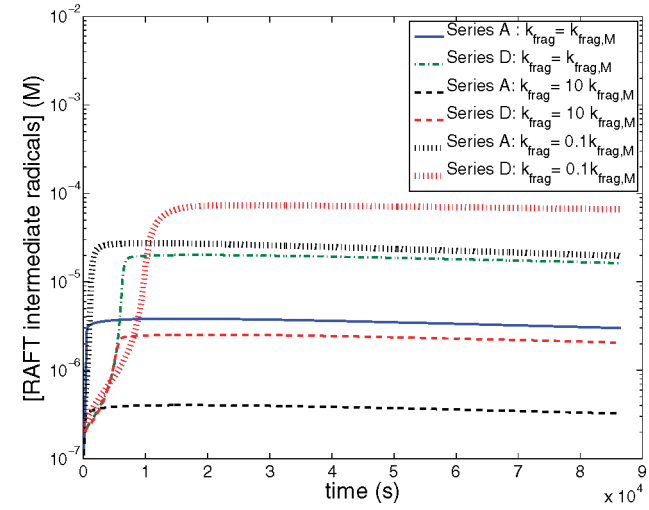

Figure 14. Behavior of the simulated intermediate radical concentration as the value of k_{frag} is varied from its best fit value. The intermediate radical concentrations vary in an approximately inversely proportional manner to the fragmentation rate.

VII. Discussion

In general, good agreement is obtained between the predictions of our model and the experimental conversion, polydispersity, and M_n data over the four polymerization reaction conditions. Although there are discrepancies between the experimental conversion/M_n data and the theoretical predictions, these are generally not systematic. The only exception being the polydispersity data, where the model tends to predict slightly lower values of the polydisperisty than the experimentally observed values, although these discrepancies may be attributed to band broadening in the SEC column.[75,76]

Moreover, the model proposed in this work correctly predicts the molecular weight distribution, as seen by the agreement with our experimental molecular weight distribution and the theoretical and experimental molecular weight distributions of Barner-Kowollik et al.[24] This is an addition to the fits between our number-average molecular weight and polydispersity index data. Similarly to the conversion, polydispersity, etc., our model correctly predicts the experimental molecular weight distribution. Our model's peaks lie directly over the experimental peaks in Figure 11 as well as predicting the correct features in the distribution. Again band

broadening appears to affect the fine details in fit of our model to the experimental molecular weight distribution. When comparing our model to the experiments and model of Barner-Kowollik et al.,[24] it is interesting to note that our model for the molecular weight distribution is as good, if not a better description of the relevant experiments on cumyl dithiobenzoate than the PREDICI simulations of Barner-Kowollik et al.[24]

The assumption of our model that cross-termination only occurs between short radicals and the RAFT intermediates is feasible, since these short radicals radicals may diffuse with greater ease compared to larger radicals, leading to a faster termination rate. Furthermore, the cross-terminated adduct of a cyanoisopropyl radical with the RAFT intermediate has been experimentally detected by MALDI-TOF mass spectrometry.[59] The model has a very large cross-termination rate coefficient, which is assumed to be the same as the termination between two short styrene radicals.[73] It is important to note that our predicted cross-termination rate coefficient is larger than the value predicted by other researchers,[26,27] although this can be rationalized since the cyanoisoproyl radical is more reactive (as suggested by the much larger rate of propagation with styrene) and diffuses with greater ease. Although our model assumes that the rate of cross-termination between the RAFT intermediate radical and long polymer chains is zero, this is an extreme example and is placed to state that the vast majority of cross-termination events occur with short chains, and long chain cross-termination is negligible. Similarly to Felderman et al.,[25] the results of our model would be unchanged if there was a long chain cross-termination rate coefficient of 10^2-10^3 L mol^{-1} s^{-1}. This would account for the small amounts of 3-armed star polymers detected,[55–58] without changing the essence of our model, namely that the majority of cross-termination occurs between *short radicals* and the RAFT intermediate.

The key feature of our model is the cross-termination of the RAFT intermediate which occurs only with *short radicals* and that the rate of fragmentation itself is slow. This mechanism of termination operating in parallel with slow fragmentation has been deduced for thioketone systems.[77,78] Although thioketones follow a different reaction scheme to the RAFT process, the thioketone species are chemically related to dithiobenzoate RAFT agents, and similarities in the radical fragmentation and termination reactions are expected. It is encouraging that our reaction scheme compares favorably to the proposed mechanism of the thioketone system, which has similar features to RAFT polymerization.

It is important to note that this model assumes that cross-termination of the RAFT intermediate radical only occurs with very short radicals; thus, we do not predict 3-armed stars in the molecular weight distribution. This assumption that smaller radicals will react more rapidly with the intermediate radical than larger radicals is intuitive and is supported by the fact that termination events are primarily diffusion controlled.[60] Although the majority of cross-terminations occur early in the reaction, because the largest population of short radicals is early in the reaction, the initiator continues to dissociate through the whole reaction, and these cross-termination events continue to occur throughout the polymerization.

The rate coefficients for addition and fragmentation of the RAFT reaction obtained by fitting the model to the data are generally consistent with a priori expectations and previous studies. In both the main equilibrium and the pre-equilibrium we obtain equilibrium constants, consistent with the slow fragmentation model for RAFT polymerization. The equilibrium constant for the pre-equilibrium is in the same order of magnitude as that predicted by Coote et al.[36] by quantum calculations. In contrast, our model predicts a smaller equilibrium constant (2×10^5) for the main equilibrium compared to the value determined by Coote et al., which is in the order of 10^7.[25,36] The difference between our main equilibrium constant and the equilibrium constant of $\sim 10^7$ predicted by Coote et al.[36] is noticeable, but the discrepancy of 1.5 orders of magnitude is plausibly explained as within the uncertainty of quantum calculations.[36]

The model's sensitivity analysis in conversion (Figures 12 which tests for sensitivity to the value of K) suggests that the equilibrium constant is accurate for our system to better than 1 order of magnitude, since variations of 1 order of magnitude in K give significant discrepancies. The sensitivity analysis on the PDI suggests that the absolute value of the PDI is mildly affected by changes of about 1 order of magnitude and greatly affected by changes of 2 orders of magnitude. This indicates that the absolute values of k_{add} and k_{frag} estimated for our system are correctly specified to within about 1 order of magnitude. Finally, we have performed a sensitivity analysis of the intermediate radical concentrations; the results of this suggest that the radical concentration is essentially inversely proportional to the equilibrium constant. However, the conversion (and propagating radical) concentrations are also very sensitive to the equilibrium constant, and decreases in K cause these values deviate far from their best fitted values.

The radical concentrations predicted by our model are essentially consistent with ESR experiments. In Figure 8 we observe propagating radical concentrations in the order of 10^{-8} M, while in Figure 7 our model shows intermediate radical concentrations in the order of $10^{-6}-10^{-5}$ M. Although the intermediate radical concentrations are higher than those in several ESR experiments[41,51] (which suggest concentrations in the order of $10^{-7}-10^{-6}$ M), our experiments are performed at higher ratios of RAFT agent to initiator and lower concentrations of AIBN. Such discrepancies may therefore be due to the exact experimental specifications and experimental uncertainties in the established ESR measurements. Although our model does not exactly reproduce the established and previously reported ESR measurements, the difference is about 1 order of magnitude, and our model has far better agreement with experimental ESR measurements as compared to other slow fragmentation models, thus marking a significant development in the understanding of RAFT kinetics. It is also important to note that this improvement in the agreement with ESR measurements is 2−3 orders of magnitude compared to the some previously published slow fragmentation models, which is remarkable in light of the fact that our discrepancy with the equilibrium constant is only 1.5 orders of magnitude from the previously determined (slow fragmenting) quantum values.

In addition to our model predicting plausible values of the intermediate radical concentrations, our model is also consistent with the experimental findings of radical storage in RAFT systems.[46] In the experiments, Barner-Kowollik et al.[46] form small radicals that initially react on the thiocarbonyl thio group to form the intermediate radical. Unlike in a polymerization system, the formation of small radicals is not continuous and ceased when the radiation is stopped and the radical is stored; therefore, little termination between small radicals and intermediate occurs, which accounts for the storage effect observed. In our model if a radical source is removed, there would be an initial phase of cross-termination; however, the majority of the short radicals would soon propagate to long chain polymers, which no longer undergo cross-termination. Furthermore, our calculations suggest slow fragmentation of the RAFT intermediate, which indicates that remaining intermediate radicals would release propagating radicals over a substantial period of time, as evinced by the large equilibrium constant of 2×10^5.

It is important to highlight one of the approximations made, which is that the current model has only a pre-equilibrium and

a main equilibrium and does not include further chain length dependence in the equilibrium constants and rate coefficients for the oligomeric species. Although chain length dependence can be important in RAFT systems,[36] this effect was not included to minimize the number of parameters to be fitted in our model. It is interesting to note that both our model and the quantum calculations show the same increasing trend in the equilibrium constant with longer chain length. The quantum calculations[36] show that the equilibrium constant increases as the number of styrene monomers increases; similarly, our calculations also indicate that the equilibrium constant increases from 10^4 in the pre-equilibrium to 2×10^5 in the main equilibrium (which has a large number of styrene monomers). It is likely that the oligomers will have equilibrium constants between those of the pre-equilibrium and the main equilibrium; that is, we expect the equilibrium constant to increase gradually from the pre-equilibrium value to the main equilibrium value as the number of monomers increases, and this trend is also predicted by the quantum calculations. This is quite a remarkable similarity between our model's results and the quantum calculations.

From our estimated rate coefficients the polymerization proceeds first by conversion of CPDB to unimeric/dimeric polymers. Once the majority of the initial RAFT agent has been converted to an oligomeric styrene polymer, the propagation proceeds further to higher degrees of polymerization. This reaction mechanism is argued since the pre-equilibrium fragmentation rate coefficient, k_{frag_l}, is larger than the main equilibrium equivalent, k_{frag_M}, by about 1 order of magnitude; in addition, the cyanoisopropyl radical propagation rate coefficient is 1 order of magnitude greater than that of styrene. The theoretical polydispersity plots show this effect, since there is an initial drop in the polydispersity as the RAFT agent converts to a unimeric polymer, and the majority of chains have one styrene unit. Following the conversion of RAFT agent to unimer, the polydispersity increases upon further polymer propagation, followed by a decrease as the *relative* difference between M_w and M_n decreases. The reaction mechanism where RAFT agent is initially converted to unimers is consistent with experimental studies on the early phase reaction kinetics. Indeed, polymerizations monitored by NMR spectroscopy showed that the RAFT agent is initially converted to unimers and dimers, before further propagation to long chain polymers.[79,80]

VIII. Conclusion

A model for RAFT polymerization kinetics is presented, which considers cross-termination between the RAFT intermediate radical and *short radicals*. The model was tested against experiments on CPDB-mediated polymerization of styrene, in the presence of AIBN, and it correctly predicted the conversion, molecular weight, and polydisperisty index over four polymerizations. The model predicts a significant equilibrium in favor of the intermediate radical rather than the free radical and the RAFT agent, which is consistent with the previously published quantum calculations and experiments. The model also predicts a significant rate coefficient for the cross-termination between the RAFT intermediate radical and the cyanoisopropyl radical. Since this model only assumes cross-termination between short radicals and the RAFT intermediate, the theoretical molecular weight distribution does not show 3-armed stars since third arm has negligible molecular weight. In addition to correctly predicting the molecular weight distribution, our model gives radical concentrations consistent with experimental ESR data. Our model is consistent with all experimental data observed to date, fits available quantum calculations, and demonstrates that the two conflicting models that have been proposed so far can actually coexist.

Acknowledgment. The authors gratefully acknowledge Wilasinee Sriprom for synthesizing the RAFT agent. The authors are grateful to Benjamin Hornby, Vincent Ladmiral, and Andrew West for fruitful discussions and experimental assistance. We thank the referees present in the review process for their constructive comments. The authors acknowledge the Australian Research Council for funding and an Australian Postdoctoral Fellowship (A.G.W.) and an Australian Postgraduate Award (D.K.).

References and Notes

(1) Veregin, R. P. N.; Georges, M. K.; Kazmaier, P. M.; Hamer, G. K. *Macromolecules* **1993**, *26*, 5316–20.
(2) Georges, M. K.; Veregin, R. P. N.; Kazmaier, P. M.; Hamer, G. K. *Macromolecules* **1993**, *26*, 2987–8.
(3) Wang, J.-S.; Matyjaszewski, K. *J. Am. Chem. Soc.* **1995**, *117*, 5614–15.
(4) Kato, M.; Kamigaito, M.; Sawamoto, M.; Higashimura, T. *Macromolecules* **1995**, *28*, 1721–3.
(5) Chiefari, J.; Chong, Y. K.; Ercole, F.; Krstina, J.; Jeffery, J.; Le, T. P. T.; Mayadunne, R. T. A.; Meijs, G. F.; Moad, C. L.; Moad, G.; Rizzardo, E.; Thang, S. H. *Macromolecules* **1998**, *31*, 5559–5562.
(6) Hawthorne, D. G.; Moad, G.; Rizzardo, E.; Thang, S. H. *Macromolecules* **1999**, *32*, 5457–5459.
(7) Perrier, S.; Takolpuckdee, P. *J. Polym. Sci., Part A: Polym. Chem.* **2005**, *43*, 5347–5393.
(8) Moad, G. *Aust. J. Chem.* **2006**, *59*, 661–662.
(9) Moad, G.; Rizzardo, E.; Thang, S. H. *Aust. J. Chem.* **2005**, *58*, 379–410.
(10) Moad, G.; Rizzardo, E.; Thang, S. H. *Aust. J. Chem.* **2006**, *59*, 669–692.
(11) Moad, G.; Mayadunne, R. T. A.; Rizzardo, E.; Skidmore, M.; Thang, S. H. *Macromol. Symp.* **2003**, *192*, 1–12.
(12) Barner, L.; Barner-Kowollik, C.; Davis, T. P.; Stenzel, M. H. *Aust. J. Chem.* **2004**, *57*, 19–24.
(13) Barner-Kowollik, C.; Davis, T. P.; Stenzel, M. H. *Aust. J. Chem.* **2006**, *59*, 719–727.
(14) Liu, B.; Kazlauciunas, A.; Guthrie, J. T.; Perrier, S. *Macromolecules* **2005**, *38*, 2131–2136.
(15) Vana, P.; Davis, T. P.; Barner-Kowollik, C. *Macromol. Rapid Commun.* **2002**, *23*, 952–956.
(16) Feldermann, A.; Stenzel, M. H.; Davis, T. P.; Vana, P.; Barner-Kowollik, C. *Macromolecules* **2004**, *37*, 2404–2410.
(17) Johnston-Hall, G.; Theis, A.; Monteiro, M. J.; Davis, T. P.; Stenzel, M. H.; Barner-Kowollik, C. *Macromol. Chem. Phys.* **2005**, *206*, 2047–2053.
(18) Lovestead, T. M.; Theis, A.; Davis, T. P.; Stenzel, M. H.; Barner-Kowollik, C. *Macromolecules* **2006**, *39*, 4975–4982.
(19) Lovestead, T. M.; Davis, T. P.; Stenzel, M. H.; Barner-Kowollik, C. *Macromol. Symp.* **2007**, *248*, 82–93.
(20) Johnston-Hall, G.; Stenzel, M. H.; Davis, T. P.; Barner-Kowollik, C.; Monteiro, M. J. *Macromolecules* **2007**, *40*, 2730–2736.
(21) Johnston-Hall, G.; Monteiro, M. J. *Macromolecules* **2008**, *41*, 727–736.
(22) Barner-Kowollik, C.; Buback, M.; Charleux, B.; Coote, M. L.; Drache, M.; Fukuda, T.; Goto, A.; Klumperman, B.; Lowe, A. B.; McLeary, J. B.; Moad, G.; Monteiro, M. J.; Sanderson, R. D.; Tonge, M. P.; Vana, P. *J. Polym. Sci., Part A: Polym. Chem.* **2006**, *44*, 5809–5831.
(23) Monteiro, M. J. *J. Polym. Sci., Part A: Polym. Chem.* **2005**, *43*, 3189–3204.
(24) Barner-Kowollik, C.; Quinn, J. F.; Morsley, D. R.; Davis, T. P. *J. Polym. Sci., Part A: Polym. Chem.* **2001**, *39*, 1353–1365.
(25) Feldermann, A.; Coote, M. L.; Stenzel, M. H.; Davis, T. P.; Barner-Kowollik, C. *J. Am. Chem. Soc.* **2004**, *126*, 15915–15923.
(26) Monteiro, M. J.; de Brouwer, H. *Macromolecules* **2001**, *34*, 349–352.
(27) Drache, M.; Schmidt-Naake, G.; Buback, M.; Vana, P. *Polymer* **2005**, *46*, 8483–8493.
(28) Buback, M.; Vana, P. *Macromol. Rapid Commun.* **2006**, *27*, 1299–1305.
(29) Buback, M.; Janssen, O.; Oswald, R.; Schmatz, S.; Vana, P. *Macromol. Symp.* **2007**, *248*, 158–167.
(30) Pallares, J.; Jaramillo-Soto, G.; Flores-Catano, C.; Vivaldo Lima, E.; Lona, L. M. F.; Penlidis, A. *J. Macromol. Sci., Pure Appl. Chem.* **2006**, *43*, 1293–1322.
(31) Prescott, S. W. *Macromolecules* **2003**, *36*, 9608–9621.
(32) Prescott, S. W.; Ballard, M. J.; Rizzardo, E.; Gilbert, R. G. *Macromol. Theory Simul.* **2006**, *15*, 70–86.
(33) Wang, A. R.; Zhu, S. *J. Polym. Sci., Part A: Polym. Chem.* **2003**, *41*, 1553–1566.
(34) Wang, A. R.; Zhu, S. *Macromol. Theory Simul.* **2003**, *12*, 196–208.
(35) Coote, M. L.; Radom, L. *J. Am. Chem. Soc.* **2003**, *125*, 1490–1491.

(36) Coote, M. L.; Krenske, E. H.; Izgorodina, E. I. *Macromol. Rapid Commun.* **2006**, *27*, 473–497.
(37) Coote, M. L.; Izgorodina, E. I.; Krenske, E. H.; Busch, M.; Barner-Kowollik, C. *Macromol. Rapid Commun.* **2006**, *27*, 1015–1022.
(38) Izgorodina, E. I.; Coote, M. L. *Chem. Phys.* **2006**, *324*, 96–110.
(39) Coote, M. L.; Barner-Kowollik, C. *Aust. J. Chem.* **2006**, *59*, 712–718.
(40) Nguyen, D. H.; Vana, P. *Aust. J. Chem.* **2006**, *59*, 549–559.
(41) Kwak, Y.; Goto, A.; Tsujii, Y.; Murata, Y.; Komatsu, K.; Fukuda, T. *Macromolecules* **2002**, *35*, 3026–3029.
(42) Goto, A.; Sato, K.; Tsujii, Y.; Fukuda, T.; Moad, G.; Rizzardo, E.; Thang, S. H. *Macromolecules* **2001**, *34*, 402–408.
(43) Perrier, S.; Barner-Kowollik, C.; Quinn, J. F.; Vana, P.; Davis, T. P. *Macromolecules* **2002**, *35*, 8300–8306.
(44) Barner-Kowollik, C.; Coote, M. L.; Davis, T. P.; Radom, L.; Vana, P. *J. Polym. Sci., Part A: Polym. Chem.* **2003**, *41*, 2828–2832.
(45) Wang, A. R.; Zhu, S.; Kwak, Y.; Goto, A.; Fukuda, T.; Monteiro, M. S. *J. Polym. Sci., Part A: Polym. Chem.* **2003**, *41*, 2833–2839.
(46) Barner-Kowollik, C.; Vana, P.; Quinn, J. F.; Davis, T. P. *J. Polym. Sci., Part A: Polym. Chem.* **2002**, *40*, 1058–1063.
(47) Tobita, H.; Yanase, F. *Macromol. Theory Simul.* **2007**, *16*, 476–488.
(48) Chaffey-Millar, H.; Stewart, D.; Chakravarty, M. M. T.; Keller, G.; Barner-Kowollik, C. *Macromol. Theory Simul.* **2007**, *16*, 575–592.
(49) Hawthorne, D. G.; Moad, G.; Rizzardo, E.; Thang, S. H. *Macromolecules* **1999**, *32*, 5457–5459.
(50) Calitz, F. M.; McLeary, J. B.; McKenzie, J. M.; Tonge, M. P.; Klumperman, B.; Sanderson, R. D. *Macromolecules* **2003**, *36*, 9687–9690.
(51) Calitz, F. M.; Tonge, M. P.; Sanderson, R. D. *Macromol. Symp.* **2003**, *193*, 277–288.
(52) Alberti, A.; Benaglia, M.; Laus, M.; Macciantelli, D.; Sparnacci, K. *Macromolecules* **2003**, *36*, 736–740.
(53) Vana, P. *Macromol. Symp.* **2007**, *248*, 71–81.
(54) Alberti, A.; Benaglia, M.; Fischer, H.; Guerra, M.; Laus, M.; Macciantelli, D.; Postma, A.; Sparnacci, K. *Helv. Chim. Acta* **2006**, *89*, 2103–2118.
(55) Kwak, Y.; Goto, A.; Fukuda, T. *Macromolecules* **2004**, *37*, 1219–1225.
(56) Kwak, Y.; Goto, A.; Komatsu, K.; Sugiura, Y.; Fukuda, T. *Macromolecules* **2004**, *37*, 4434–4440.
(57) Venkatesh, R.; Staal, B. B. P.; Klumperman, B.; Monteiro, M. J. *Macromolecules* **2004**, *37*, 7906–7917.
(58) Geelen, P.; Klumperman, B. *Macromolecules* **2007**, *40*, 3914–3920.
(59) Bathfield, M.; D'Agosto, F.; Spitz, R.; Ladaviere, C.; Charreyre, M.-T.; Delair, T. *Macromol. Rapid Commun.* **2007**, *28*, 856–862.
(60) Heuts, J. P. A.; Russell, G. T.; Smith, G. B.; van Herk, A. M. *Macromol. Symp.* **2007**, *248*, 12–22.
(61) Gallot-Grubisic, Z.; Rempp, P.; Benoit, H. *J. Polym. Sci., Polym. Lett. Ed.* **1967**, *5*, 753–9.
(62) Thang, S. H.; Chong, Y. K.; Mayadunne, R. T. A.; Moad, G.; Rizzardo, E. *Tetrahedron Lett.* **1999**, *40*, 2435–2438.
(63) Smith, G. B.; Russell, G. T.; Heuts, J. P. A. *Macromol. Theory Simul.* **2003**, *12*, 299–314.
(64) Gardiner, C. W. *Handbook of Stochastic Methods for Physics, Chemistry, and the Natural Sciences*, 3rd ed.; Springer-Verlag: Berlin, 2004.
(65) Flory, P. J. *Principles of Polymer Chemistry*; Cornell University Press: Ithaca, NY, 1953.
(66) Clay, P. A.; Gilbert, R. G. *Macromolecules* **1995**, *28*, 552–69.
(67) Press, W. H.; Teukolsky, S. A.; Vetterling, W. T.; Flannery, B. P. *Numerical Recipes in FORTRAN*, 2nd ed.; Cambridge University Press: Cambridge, 1992.
(68) Dekker, K.; Verwer, J. G. *Stability of Runge-Kutta Methods for Stiff Nonlinear Differential Equations*; Elsevier Science Publishers B.V.: Amsterdam, 1984.
(69) Buback, M.; Huckestein, B.; Kuchta, F.-D.; Russell, G. T.; Schmid, E. *Macromol. Chem. Phys.* **1994**, *195*, 2117–40.
(70) Moad, G.; Rizzardo, E.; Solomon, D. H.; Johns, S. R.; Willing, R. I. *Makromol. Chem. Rapid Commun.* **1984**, *5*, 793–8.
(71) Heuts, J. P. A.; Russell, G. T. *Eur. Polym. J.* **2006**, *42*, 3–20.
(72) Buback, M.; Garcia-Rubio, L. H.; Gilbert, R. G.; Napper, D. H.; Guillot, J.; Hamielec, A. E.; Hill, D.; O'Driscoll, K. F.; Olaj, O. F.; Shen, J.; Solomon, D.; Moad, G.; Stickler, M.; Tirrell, M.; Winnik, M. A. *J. Polym. Sci., Part C: Polym. Lett.* **1988**, *26*, 293–7.
(73) Olaj, O. F.; Vana, P. *J. Polym. Sci., Part A: Polym. Chem.* **2000**, *38*, 697–705.
(74) Kothe, T.; Marque, S.; Martschke, R.; Popov, M.; Fischer, H. *J. Chem. Soc., Perkin Trans. 2* **1998**, 1553–1559.
(75) Baumgarten, J. L.; Busnel, J. P.; Meira, G. R. *J. Liq. Chromatogr. Relat. Technol.* **2002**, *25*, 1967–2001.
(76) Konkolewicz, D.; Taylor, J. W., II; Castignolles, P.; Gray-Weale, A.; Gilbert, R. G. *Macromolecules* **2007**, *40*, 3477–3487.
(77) Toy, A. A.; Chaffey-Millar, H.; Davis, T. P.; Stenzel, M. H.; Izgorodina, E. I.; Coote, M. L.; Barner-Kowollik, C. *Chem. Commun.* **2006**, 835–837.
(78) Junkers, T.; Stenzel, M. H.; Davis, T. P.; Barner-Kowollik, C. *Macromol. Rapid Commun.* **2007**, *28*, 746–753.
(79) McLeary, J. B.; Tonge, M. P.; Klumperman, B. *Macromol. Rapid Commun.* **2006**, *27*, 1233–1240.
(80) Tonge, M. P.; Calitz, F. M.; Sanderson, R. D. *Macromol. Chem. Phys.* **2006**, *207*, 1852–1860.

MA800388C